



RECEIVED  
20 February 2024

REVISED  
1 April 2024

ACCEPTED FOR PUBLICATION  
9 April 2024

PUBLISHED  
18 April 2024

# Abundant optical soliton solutions to the fractional perturbed Chen-Lee-Liu equation with conformable derivative

Aminul Islam , Md. Sagib , Md. Mamunur Rashid and Md. Al Amin

Department of Mathematics, Hajee Mohammad Danesh Science and Technology University, Dinajpur-5200, Bangladesh

E-mail: [sagib.mat@tch.hstu.ac.bd](mailto:sagib.mat@tch.hstu.ac.bd)

**Keywords:** improved tanh method, perturbed Chen-Lee-Liu model, conformable derivative, optical soliton

## Abstract

This research focuses on the space-time fractional nonlinear perturbed Chen-Lee-Liu model, which describes the propagation behavior of optical pulses in the fields of optical fiber and plasma. The equation is considered with respect to the conformable derivative, and a composite fractional wave transformation is employed to reformulate it into a nonlinear equation with a single variable. The improved tanh method has been applied to derive novel analytical wave solutions for the given equation. Consequently, various types of solitonic wave patterns emerge, including but not limited to periodic, bell-shaped, anti-bell-shaped, V-shaped, kink, and compacton solitonic structures. The acquired solutions could potentially aid in the analysis of signal transmission in optical fibers and the characterization of plasma properties. The physical interpretations of the solutions are investigated using three-dimensional surface plots and two-dimensional density plots. Additionally, combined two-dimensional plots are being used to discuss the effects of the order of the fractional derivative on the generated wave patterns. Moreover, this study demonstrates the efficacy and reliability of the chosen technique.

## 1. Introduction

Many scientists in the illustrious age of scientific progress and technological innovation employed fractional order nonlinear partial differential equations (FNPDEs) to analyze intricate mathematical models that arise in the fields of plasma physics, optical fibers, fluid dynamics, quantum mechanics, neuroscience, robotics, and others. Therefore, in order to overcome the initial obstacles, it is rational to identify the wave solutions obtained through the analysis of these models and provide a theoretical description of the phenomenon. The mathematical solutions for waves obtained through analytical methods of the FNDEs facilitate the investigation of complicated topics more successfully than the solutions of equations with integer orders. Russell found the long wave within the Union Canal in 1834. He discovered that a solitary wave could travel a great distances while maintaining an unchanging configuration and velocity. The acquisition of soliton solutions for important equations is now a highly researched field among academics. A number of scholars have provided justification for a variety of sophisticated methods to investigate soliton solutions, including the Hirota's process [1], the sine-Gordon expansion technique [2, 3], the first-integral approach [4, 5], the auxiliary equation technique [6, 7], the sine-cosine scheme [8, 9], and the generalized Kudryashov procedure [10, 11], the  $(G'/G)$ -expansion approach [12, 13], the extended tanh-function scheme [14, 15], the  $\phi^6$ -model expansion method [16], the Jacobi-elliptic function expansion technique [17, 18], the exponent function process [19], the  $(G'/G, 1/G)$ -expansion method [20, 21], the generalized  $(G'/G)$ -expansion technique [22], the modified extended tanh-function method [23, 24], and many others.

The transmission of short pulses in fiber optic cables is a highly intriguing subject that attracts both experimental and theoretical research. The fundamental aspects of this phenomenon are elucidated through the nonlinear Schrödinger equation (NSE). The quest for soliton solutions of the NSE has emerged as a prominent subject across diverse scientific domains, including signal propagation through fiber optic cables, plasma

physics, and quantum mechanics [25]. The NSE, along with its diverse modifications, serves as a foundational model for investigating the dynamics of sub-microscopic particles like photons and revealing the impacts of higher-order nonlinear effects in real-world physical systems [26]. For instance, the nonlocal Kundu-NSE, which arises in nonlocal symmetry, is a modification of NSE and is utilized for modeling wave propagation in dispersive media [27]. Again, derivative nonlinear Schrödinger (DNS) type equations have significant applications in plasma physics and nonlinear optics, such as the mixed Chen-Lee-Liu DNS equation, which can depict the transmission of localized structures within the nonlinear dispersive medium [28].

Various models describe the dynamics of soliton propagation via optical waveguides, encompassing fibers, optical couplers, meta-materials, and other structures. One notable model among these is the nonlinear Chen-Lee-Liu (CLL) equation, which garners significant attention in nonlinear optics research. The CLL equation characterizes the behavior of light propagation in nonlinear optical fibers and can also manifest in optical couplers, meta-materials, and optoelectronic devices [29]. Since the inception of the CLL equation, numerous scholars have proposed and investigated various iterations of this equation. Among these iterations, the integer-ordered perturbed CLL equation [29] takes the subsequent structure:

$$i\frac{\partial q}{\partial t} + \alpha\frac{\partial^2 q}{\partial x^2} + i\beta|q|^2\frac{\partial q}{\partial x} = i\left[\eta\frac{\partial q}{\partial x} + \gamma\frac{\partial}{\partial x}(|q|^{2m}q) + \kappa\left(\frac{\partial(|q|^{2m})}{\partial x}\right)q\right]. \quad (1.1)$$

The perturbed CLL equation finds utility across various domains, ranging from investigating optical soliton behavior and analyzing the nonlinear interactions within fiber optic cables for the development of control systems resilient to minor disturbances and examining the stability and features for chaotic systems. Moreover, in the realm of plasma physics, this equation serves as a tool to explore electromagnetic wave propagation, nonlinear dynamics of wave-particle interactions, and contributes to advancements in scientific endeavors leveraging plasma technologies [30]. The soliton solutions of CLL equation and its various modifications were studied by several researchers through different approaches, such as the generalized exponential rational function method [31], the enhanced Kudryashov's [32], the modified extended auxiliary equation mapping method [33], the extended simplest equation method [34] and others [35, 36].

The solitary wave solutions of the perturbed space-time fractional nonlinear Chen-Lee-Liu equation are investigated for  $m = 1$  in this research [25]:

$$iD_x^\sigma q + \alpha D_{xx}^{2\sigma} q + i\beta|q|^2 D_x^\sigma q = i[\eta D_x^\sigma q + \gamma D_x^\sigma (|q|^2 q) + \kappa(D_x^\sigma (|q|^2))q], \quad 0 < \sigma \leq 1. \quad (1.2)$$

In equation (1.2),  $q = q(x, t)$  is the complex wave function of spatial and temporal variables  $x$  and  $t$  respectively,  $\alpha$  is the dissipation coefficient,  $\beta$  and  $\kappa$  are nonlinear dispersion coefficients,  $\eta$  is the coefficient of inter model dispersion,  $\gamma$  is the parameter of shelf-stepping,  $\sigma$  is the order of the conformable fractional derivative which lies between  $(0, 1]$ . It can elucidate the evolution and interactions of pulses as they propagate within a given interval, illustrating how nonlinear phenomena and other influences give rise to diverse wave patterns over time at each location within the specified interval.

The soliton solutions of equation (1.2) have garnered considerable attention from academics in recent years due to its profound influence on fiber optic cable and plasma physics. Until now, only a few studies have been conducted on the space-time fractional perturbed nonlinear CLL equation. Martínez *et al* [25] obtained analytical soliton solutions for the model (1.2) using the modified exp  $(-\phi(\xi))$ -expansion function method by introducing a new local fractional derivative. Khatun and Akbar [30] used  $(G'/G, 1/G)$ -expansion method to derive some new optical solitons for the CLL equation (1.2) with Atangana's beta derivative. The beta fractional perturbed CLL model was studied by Tripathy and Sahoo [37] to study the distinct optical solutions. Furthermore, new optical solitons of the perturbed CLL equation in conjunction with a novel local fractional derivative were derived by Ouahid *et al* [38].

Fractional calculus is currently widely used to explore novel properties of solitons. More appropriate analysis of physical phenomena with higher degrees of freedom is possible using fractional models. This approach significantly impacts the formation of solitons with various shapes and high intensities. Researchers are currently engaged in the exploration of fractional calculus, where they are developing novel operators including the Riemann-Liouville, Caputo, Atangana Baleanu and Caputo Fabrizio derivatives. Among these, the conformable fractional operator emerges as a promising advancement, addressing certain limitations inherent in existing fractional operators. It exhibits qualities akin to traditional calculus, facilitating operations such as the derivative of a quotient of functions, chain rule, and the product of functions, as well as principles like the mean value theorem and Rolle's theorem. The application of the conformable derivative is characterized by its simplicity and effectiveness, offering insights into the behavior of various physical phenomena. Particularly beneficial in tackling complex models, this derivative enhances convenience in modeling numerous physical problems. Differential equations involving the conformable fractional derivative are notably easier to solve compared to those involving the Caputo or Riemann-Liouville fractional derivative, underscoring its utility and versatility in scientific inquiry.

To the extent of our understanding, the improved tanh method [39, 40] has not been employed yet in investigating the space-time fractional perturbed CLL equation alongside the conformable derivative [41]. Therefore, the goal of this study is to utilize the improved tanh method to uncover novel findings for the aforementioned equation. Consequently, numerous new exact traveling wave solutions, such as periodic, bell-shaped, V-shaped, anti-bell-shaped, kink, and compacton, employing diverse sets of free parameters, have been obtained. Furthermore, we will observe that varying the order of the conformable derivative can alter the dynamics of soliton waves, providing additional insights into propagating waves. Additionally, non-regular oscillatory phenomena will be observed in the conformable fractional model (1.2) compared to its integer case. For the above results and the simplicity of the conformable fractional derivative, we are motivated to analyze the model (1.2) in the sense conformable derivative. One of the advantages of the proposed method over alternative approaches is its capability to yield a greater number of arbitrary constants and various types of solutions. In addition to its fundamental application, it also assists numerical solvers in verifying the accuracy of their results and facilitates stability analysis.

The remainder of the document will be structured as follows: section 2 represents the methodology and features of the conformable derivative. Section 3 introduces the implementation of the improved tanh technique. Section 4 provides a concise discussion accompanied by graphical illustrations. In section 5, we present a comparison between our extracted solutions and existing literature, and lastly, conclusions are drawn in section 6.

## 2. Preliminaries and methodology

### 2.1. Conformal derivative

The conformable fractional order derivative of  $q(\zeta)$  is given by

$$D_{\zeta}^{\sigma}(q(\zeta)) = \lim_{\epsilon \rightarrow 0} \frac{q(\zeta + \epsilon \zeta^{1-\sigma}) - q(\zeta)}{\epsilon}, \text{ where } 0 < \sigma \leq 1.$$

Suppose that the functions  $q = q(\zeta)$  and  $r = r(\zeta)$  are  $\sigma$ -differentiable at  $\zeta > 0$  with  $\sigma \in (0, 1]$ , then the conformable derivative [41] satisfies the following properties:

- (i)  $D_{\zeta}^{\sigma}(\zeta^n) = n\zeta^{n-\sigma}$ ,  $\forall n \in \mathbb{R}$ .
- (ii)  $D_{\zeta}^{\sigma}(c) = 0$ .
- (iii)  $D_{\zeta}^{\sigma}(aq + br) = aD_{\zeta}^{\sigma}(q) + bD_{\zeta}^{\sigma}(r)$ ,  $\forall a, b \in \mathbb{R}$ .
- (iv)  $D_{\zeta}^{\sigma}(qr) = qD_{\zeta}^{\sigma}(r) + rD_{\zeta}^{\sigma}(q)$ .
- (v)  $D_{\zeta}^{\sigma}(q/r) = \frac{rD_{\zeta}^{\sigma}(q) - qD_{\zeta}^{\sigma}(r)}{r^2}$ .
- (vi)  $D_{\zeta}^{\sigma}(q)(\zeta) = \zeta^{1-\sigma} \frac{dq}{d\zeta}$ .
- (vii)  $D_{\zeta}^{\sigma}(qor)(\zeta) = \zeta^{1-\sigma} r'(\zeta) q'(\zeta)$ .

### 2.2. The improved tanh method

Consider the fractional order nonlinear partial differential equation with unknown function  $q(x_1, x_2, x_3, \dots, x_n, t)$  as:

$$\Phi(q, D_t^{\alpha} q, D_{x_1}^{\alpha} q, D_{tt}^{2\alpha} q, D_{x_1 x_1}^{2\alpha} q, \dots) = 0, \quad 0 < \alpha \leq 1, \quad (2.1)$$

where  $\Phi$  represent a polynomial in  $q$  and its all fractional order partial derivatives. Take traveling wave transformation for real equations as follows:

$$q = q(x_1, x_2, x_3, \dots, x_n, t) = Q(\zeta), \quad \zeta = \zeta(x_1, x_2, x_3, \dots, x_n, t), \quad (2.2)$$

or define traveling wave transformation for complex equation as:

$$q = q(x_1, x_2, x_3, \dots, x_n, t) = Q(\zeta)e^{i\theta}, \quad \zeta = \zeta(x_1, x_2, x_3, \dots, x_n, t), \quad \theta = \theta(x_1, x_2, x_3, \dots, x_n, t). \quad (2.3)$$

The equation (2.1) with the help of (2.2) is turned into the ordinary differential equation as:

$$\Phi(Q, Q', Q'', Q''', \dots) = 0, \quad (2.4)$$

where primes in  $Q$  define the order of derivative due to the variable  $\zeta$ . Differentiating (2.4) as much as needed and set the constants of integration equal to zero for adopting soliton solutions. The improved tanh technique suggests us to adopt the form of solution as:

$$Q(\zeta) = \frac{\sum_{i=0}^N \iota_i \Omega^i(\zeta) + \sum_{j=1}^N \tau_j \Omega^{-j}(\zeta)}{\sum_{i=0}^N \epsilon_i \Omega^i(\zeta) + \sum_{j=1}^N \varepsilon_j \Omega^{-j}(\zeta)}, \quad (2.5)$$

where the constant  $\iota_i$ ,  $\tau_j$ ,  $\epsilon_i$ , and  $\varepsilon_j$  ( $i, j = 0, 1, \dots, N$ ) are determined later and  $\Omega(\zeta)$  satisfies the auxiliary equation,

$$\Omega'(\zeta) = \delta + \Omega^2(\zeta). \quad (2.6)$$

The equation (2.5) gives the following group of solutions.

Solution group I: when  $\delta < 0$

$$\Omega(\zeta) = -\sqrt{-\delta} \tanh(\sqrt{-\delta} \zeta) \quad (2.7)$$

$$\Omega(\zeta) = -\sqrt{-\delta} \coth(\sqrt{-\delta} \zeta) \quad (2.8)$$

Solution group II: when  $\delta = 0$

$$\Omega(\zeta) = -1/\zeta \quad (2.9)$$

Solution group III: when  $\delta > 0$

$$\Omega(\zeta) = \sqrt{\delta} \tan(\sqrt{\delta} \zeta) \quad (2.10)$$

$$\Omega(\zeta) = -\sqrt{\delta} \cot(\sqrt{\delta} \zeta) \quad (2.11)$$

When (2.5) and (2.6) are used in (2.4), it becomes a polynomial in  $\Omega$ , and equating the coefficients of  $\Omega$  to zero produces a set of algebraic equations. These equations can be solved for unknown parameters by using any computational software. Substituting the the values of unknown parameters along with the solution of (2.6) in (2.5), we obtain the analytical wave solutions of (2.1).

### 3. Extraction of soliton solutions

Assume that the wave variable transformation is defined by

$$q(x, t) = e^{i\Theta} Q(\zeta), \text{ where } \Theta = a\frac{x^\sigma}{\sigma} + b\frac{t^\sigma}{\sigma} \text{ and } \zeta = c\frac{x^\sigma}{\sigma} + d\frac{t^\sigma}{\sigma}. \quad (3.1)$$

With the help of the transformation (3.1), the CLL model (1.2) can be transformed into the subsequent complex nonlinear equation:

$$(-b - a(\alpha a - \eta))Q(\zeta) + (\gamma - \beta)aQ^3(\zeta) + i(d + 2\alpha ac - \eta c)Q'(\zeta) + i(\beta - 3\gamma - 2\kappa)cQ^2(\zeta)Q'(\zeta) + \alpha c^2Q''(\zeta) = 0. \quad (3.2)$$

Equating the real and imaginary parts from both sides of the equation (3.2), we respectively reached at

$$(-b - a(\alpha a - \eta))Q(\zeta) + (\gamma - \beta)aQ^3(\zeta) + \alpha c^2Q''(\zeta) = 0 \quad (3.3)$$

and

$$(d + 2\alpha ac - \eta c)Q'(\zeta) + (\beta - 3\gamma - 2\kappa)cQ^2(\zeta)Q'(\zeta) = 0. \quad (3.4)$$

Taking integration on (3.4), the following results are yielded:

$$d = -2\alpha ac + \eta c \text{ and } \beta = 3\gamma + 2\kappa \quad (3.5)$$

Then the equation (3.3) is expected to be solved. Applying the principle of homogeneous balance in equation (3.3) provides  $N = 1$ . Therefore, the assumed solution of equation (3.3) can be written in the following form:

$$Q(\zeta) = \frac{\iota_0 + \iota_1 \Omega(\zeta) + \tau_1 \Omega^{-1}(\zeta)}{\epsilon_0 + \epsilon_1 \Omega(\zeta) + \varepsilon_1 \Omega^{-1}(\zeta)} \quad (3.6)$$

Now, using (3.6) and its necessary derivatives in (3.3) provides a polynomial in  $\Omega(\zeta)$ . Then, collecting the coefficients of different powers of  $Q$  and then set them to zero gives us a system of algebraic equations. Solving the obtained system using mathematical software MAPLE offers us seven sets of solutions. These solution sets and their corresponding contributions to the unknown function  $q(x, t)$  are explained below.

Set 1:

$$b = 2\alpha c^2\delta - \alpha a^2 + \eta a, \quad \iota_0 = \iota_1 = \varepsilon_1 = 0, \quad \epsilon_0 = \pm \frac{\sqrt{\alpha a(\gamma + \kappa)}}{\alpha \delta c} \tau_1, \quad \epsilon_1 = 0$$

Agreeing to this set, we get the exact solution of equation (3.3) along with the considering solution (3.6) as:

$$Q(\zeta) = \pm \frac{\alpha\delta c}{\Omega(\zeta)\sqrt{\alpha a(\gamma + \kappa)}}. \quad (3.7)$$

If the solution obtained by the improved tanh method for  $\Omega(\zeta)$  of the solution group I, i.e. when  $\delta < 0$ , introduce  $\Omega(\zeta) = -\sqrt{-\delta} \tanh(\sqrt{-\delta}\zeta)$  in equation (3.7), and takes necessary simplification, the following soliton solution is obtained:

$$Q(\zeta) = \pm \frac{\sqrt{-\delta} \alpha c}{\tanh(\sqrt{-\delta}\zeta)\sqrt{\alpha a(\gamma + \kappa)}} \quad (3.8)$$

along with  $\zeta = c\frac{x^\sigma}{\sigma} + (-2\alpha ac + \eta c)\frac{t^\sigma}{\sigma}$ .

Now, substituting  $Q(\zeta)$  in equation (3.1), our required analytical solution of the fractional perturbed CLL nonlinear equation (1.2) by the improved tanh method is

$$q_1^1(x, t) = \pm \frac{\sqrt{-\delta} \alpha c}{\tanh(\sqrt{-\delta}\zeta)\sqrt{\alpha a(\gamma + \kappa)}} e^{i\Theta}, \delta < 0, \quad (3.9)$$

where  $\Theta = a\frac{x^\sigma}{\sigma} + (2\alpha c^2\delta - \alpha a^2 + \eta a)\frac{t^\sigma}{\sigma}$ .

By performing a similar process as in (3.9), we obtain other solutions of this set as:

$$q_1^2 = \pm \frac{\sqrt{-\delta} \alpha c}{\coth(\sqrt{-\delta}\zeta)\sqrt{\alpha a(\gamma + \kappa)}} e^{i\Theta}, \delta < 0, \quad (3.10)$$

$$q_1^3 = \pm \frac{\sqrt{\delta} \alpha c}{\tan(\sqrt{\delta}\zeta)\sqrt{\alpha a(\gamma + \kappa)}} e^{i\Theta}, \delta > 0, \quad (3.11)$$

$$q_1^4 = \mp \frac{\sqrt{\delta} \alpha c}{\cot(\sqrt{\delta}\zeta)\sqrt{\alpha a(\gamma + \kappa)}} e^{i\Theta}, \delta > 0, \quad (3.12)$$

where  $\Theta = a\frac{x^\sigma}{\sigma} + (2\alpha c^2\delta - \alpha a^2 + \eta a)\frac{t^\sigma}{\sigma}$  and  $\zeta = c\frac{x^\sigma}{\sigma} + (-2\alpha ac + \eta c)\frac{t^\sigma}{\sigma}$ .

Set 2:

$$b = -4\alpha c^2\delta - a^2\alpha + a\eta, \iota_0 = \epsilon_0 = 0, \iota_1 = \pm \frac{2\sqrt{a(\gamma + \kappa)\alpha\delta} \epsilon_1 c}{a(\gamma + \kappa)}, \tau_1 = \pm \frac{2\delta\sqrt{a(\gamma + \kappa)\alpha\delta} \epsilon_1 c}{a(\gamma + \kappa)}, \varepsilon_1 = -\delta\epsilon_1$$

Considering this set, using the same process executed for set 1, the solutions for this set are:

$$q_2^1 = \mp \frac{2\sqrt{a(\gamma + \kappa)\alpha\delta} c}{a(\gamma + \kappa)(2(\cosh^2(\sqrt{-\delta}\zeta)) - 1)} e^{i\Theta}, \delta < 0 \quad (3.13)$$

$$q_2^2 = \pm \frac{2\sqrt{a(\gamma + \kappa)\alpha\delta} c}{a(\gamma + \kappa)(2(\cosh^2(\sqrt{-\delta}\zeta)) - 1)} e^{i\Theta}, \delta < 0 \quad (3.14)$$

$$q_2^3 = \mp \frac{2\sqrt{a(\gamma + \kappa)\alpha\delta} c}{a(\gamma + \kappa)(2(\cos^2(\sqrt{\delta}\zeta)) - 1)} e^{i\Theta}, \delta > 0 \quad (3.15)$$

$$q_2^4 = \pm \frac{2\sqrt{a(\gamma + \kappa)\alpha\delta} c}{a(\gamma + \kappa)(2(\cos^2(\sqrt{\delta}\zeta)) - 1)} e^{i\Theta}, \delta > 0 \quad (3.16)$$

where  $\Theta = a\frac{x^\sigma}{\sigma} + (-4\alpha c^2\delta - a^2\alpha + a\eta)\frac{t^\sigma}{\sigma}$  and  $\zeta = c\frac{x^\sigma}{\sigma} + (-2\alpha ac + \eta c)\frac{t^\sigma}{\sigma}$ .

Set 3:

$$b = 2\alpha c^2\delta - \alpha a^2 + \eta a, \iota_0 = \tau_1 = \epsilon_1 = \varepsilon_1 = 0, \epsilon_0 = \pm \frac{\sqrt{\alpha a(\gamma + \kappa)} \iota_1}{\alpha c}$$

Corresponding to this set, the wave solutions are:

$$q_3^1 = \mp \frac{\sqrt{-\delta} \tanh(\sqrt{-\delta}\zeta)\alpha c}{\sqrt{\alpha a(\gamma + \kappa)}} e^{i\Theta}, \delta < 0 \quad (3.17)$$

$$q_3^2 = \mp \frac{\sqrt{-\delta} \coth(\sqrt{-\delta}\zeta)\alpha c}{\sqrt{\alpha a(\gamma + \kappa)}} e^{i\Theta}, \delta < 0 \quad (3.18)$$

$$q_3^3 = \mp \frac{\alpha c}{\zeta\sqrt{\alpha a(\gamma + \kappa)}} e^{i\Theta}, \delta = 0 \quad (3.19)$$

$$q_3^4 = \pm \frac{\sqrt{\delta} \tan(\sqrt{\delta} \zeta) \alpha c}{\sqrt{\alpha a(\gamma + \kappa)}} e^{i\Theta}, \delta > 0 \quad (3.20)$$

$$q_3^5 = \mp \frac{\sqrt{\delta} \cot(\sqrt{\delta} \zeta) \alpha c}{\sqrt{\alpha a(\gamma + \kappa)}} e^{i\Theta}, \delta > 0 \quad (3.21)$$

where  $\Theta = a \frac{x^\sigma}{\sigma} + (2\alpha c^2 \delta - \alpha a^2 + \eta a) \frac{t^\sigma}{\sigma}$  and  $\zeta = c \frac{x^\sigma}{\sigma} + (-2\alpha a c + \eta c) \frac{t^\sigma}{\sigma}$ .

Set 4:

$$b = -4\alpha c^2 \delta - \alpha a^2 + \eta a, \iota_0 = \epsilon_1 = \varepsilon_1 = 0, \epsilon_0 = \pm \frac{\sqrt{\alpha a(\gamma + \kappa)} \iota_1}{\alpha c}, \tau_1 = \delta \iota_1$$

For this set, we have:

$$q_4^1 = \pm \frac{\alpha c \sqrt{-\delta}}{\sqrt{\alpha a(\gamma + \kappa)} \cosh(\sqrt{-\delta} \zeta) \sinh(\sqrt{-\delta} \zeta)} e^{i\Theta}, \delta < 0 \quad (3.22)$$

$$q_4^2 = \mp \frac{\alpha c \sqrt{-\delta}}{\sqrt{\alpha a(\gamma + \kappa)} \cosh(\sqrt{-\delta} \zeta) \sinh(\sqrt{-\delta} \zeta)} e^{i\Theta}, \delta < 0 \quad (3.23)$$

$$q_4^3 = \mp \frac{(\zeta^2 \delta + 1) \alpha c}{\zeta \sqrt{\alpha a(\gamma + \kappa)}} e^{i\Theta}, \delta = 0 \quad (3.24)$$

$$q_4^4 = \pm \frac{\alpha c \sqrt{\delta}}{\sqrt{\alpha a(\gamma + \kappa)} \cos(\sqrt{\delta} \zeta) \sin(\sqrt{\delta} \zeta)} e^{i\Theta}, \delta > 0 \quad (3.25)$$

$$q_4^5 = \mp \frac{\alpha c \sqrt{\delta}}{\sqrt{\alpha a(\gamma + \kappa)} \cos(\sqrt{\delta} \zeta) \sin(\sqrt{\delta} \zeta)} e^{i\Theta}, \delta > 0 \quad (3.26)$$

where  $\Theta = a \frac{x^\sigma}{\sigma} + (-4\alpha c^2 \delta - a^2 \alpha + a \eta) \frac{t^\sigma}{\sigma}$  and  $\zeta = c \frac{x^\sigma}{\sigma} + (-2\alpha a c + \eta c) \frac{t^\sigma}{\sigma}$ .

Set 5:

$$b = 8\alpha c^2 \delta - \alpha a^2 + \eta a, \iota_0 = \epsilon_1 = \varepsilon_1 = 0, \epsilon_0 = \pm \frac{\sqrt{\alpha a(\gamma + \kappa)} \iota_1}{\alpha c}, \tau_1 = -\delta \iota_1$$

With this set, we proceed as:

$$q_5^1 = \mp \frac{(\tanh^2(\sqrt{-\delta} \zeta) + 1) \alpha c \sqrt{-\delta}}{\tanh(\sqrt{-\delta} \zeta) \sqrt{\alpha a(\gamma + \kappa)}} e^{i\Theta}, \delta < 0 \quad (3.27)$$

$$q_5^2 = \mp \frac{(\coth^2(\sqrt{-\delta} \zeta) + 1) \alpha c \sqrt{-\delta}}{\coth(\sqrt{-\delta} \zeta) \sqrt{\alpha a(\gamma + \kappa)}} e^{i\Theta}, \delta < 0 \quad (3.28)$$

$$q_5^3 = \pm \frac{(\zeta^2 \delta - 1) \alpha c}{\zeta \sqrt{\alpha a(\gamma + \kappa)}} e^{i\Theta}, \delta = 0 \quad (3.29)$$

$$q_5^4 = \pm \frac{\sqrt{\delta} (\tan^2(\sqrt{\delta} \zeta) - 1) \alpha c}{\tan(\sqrt{\delta} \zeta) \sqrt{\alpha a(\gamma + \kappa)}} e^{i\Theta}, \delta > 0 \quad (3.30)$$

$$q_5^5 = \mp \frac{\sqrt{\delta} (\cot^2(\sqrt{\delta} \zeta) - 1) \alpha c}{\cot(\sqrt{\delta} \zeta) \sqrt{\alpha a(\gamma + \kappa)}} e^{i\Theta}, \delta > 0 \quad (3.31)$$

where  $\Theta = a \frac{x^\sigma}{\sigma} + (8\alpha c^2 \delta - \alpha a^2 + \eta a) \frac{t^\sigma}{\sigma}$  and  $\zeta = c \frac{x^\sigma}{\sigma} + (-2\alpha a c + \eta c) \frac{t^\sigma}{\sigma}$ .

Set 6:

$$b = 2\alpha c^2 \delta - \alpha a^2 + \eta a, \iota_0 = 0, \epsilon_0 = \pm \frac{\alpha c^2 \delta \epsilon_1^2 + a \iota_1^2 \gamma + a \iota_1^2 \kappa}{\sqrt{a \alpha \gamma + a \alpha \kappa} \iota_1 c}, \tau_1 = -\frac{\alpha c^2 \delta^2 \epsilon_1^2}{a \iota_1 (\gamma + \kappa)}, \varepsilon_1 = \delta \epsilon_1$$

So, the exact solutions for this set are:

$$q_6^1 = \pm \frac{c (\Upsilon^2 a \iota_1^2 (\gamma + \kappa) + \alpha c^2 \delta \epsilon_1^2) \delta \sqrt{a \alpha (\gamma + \kappa)}}{(\gamma + \kappa) (\pm c \delta \iota_1 \epsilon_1 (\Upsilon - 1) (\Upsilon + 1) \sqrt{a \alpha (\gamma + \kappa)} + (-(-\delta)^{\frac{3}{2}} c^2 \alpha \epsilon_1^2 + a \sqrt{-\delta} \iota_1^2 (\gamma + \kappa)) \Upsilon) a}, \delta < 0 \quad (3.32)$$

$$q_6^2 = \pm \frac{\delta \sqrt{a \alpha (\gamma + \kappa)} (\Pi^2 a \iota_1^2 (\gamma + \kappa) + \alpha c^2 \delta \epsilon_1^2) c}{a (\pm c \delta \iota_1 \epsilon_1 (\Pi - 1) (\Pi + 1) \sqrt{a \alpha (\gamma + \kappa)} + \Pi (-(-\delta)^{\frac{3}{2}} c^2 \alpha \epsilon_1^2 + a \sqrt{-\delta} \iota_1^2 (\gamma + \kappa))) (\gamma + \kappa)}, \delta < 0 \quad (3.33)$$

$$q_6^3 = \mp \frac{c\sqrt{a\alpha(\gamma + \kappa)}(a\iota_1^2(\gamma + \kappa) - \alpha c^2\delta^2\epsilon_1^2\zeta^2)e^{i\Theta}}{a(\mp c\iota_1\epsilon_1(\zeta^2\delta + 1)\sqrt{a\alpha(\gamma + \kappa)} + (a\iota_1^2(\gamma + \kappa) + \alpha c^2\delta\epsilon_1^2)\zeta)(\gamma + \kappa)}, \delta = 0 \quad (3.34)$$

$$q_6^4 = \pm \frac{((\tan^2(\sqrt{\delta}\zeta))a\iota_1^2(\gamma + \kappa) - \alpha c^2\delta\epsilon_1^2)\sqrt{a\alpha(\gamma + \kappa)} c\delta e^{i\Theta}}{(\pm c\delta\iota_1\epsilon_1(\tan^2(\sqrt{\delta}\zeta) + 1)\sqrt{a\alpha(\gamma + \kappa)} + \tan(\sqrt{\delta}\zeta)(\delta^{\frac{3}{2}}\alpha c^2\epsilon_1^2 + a\sqrt{\delta}\iota_1^2(\gamma + \kappa)))(\gamma + \kappa)a}, \delta > 0 \quad (3.35)$$

$$q_6^5 = \mp \frac{((\cot^2(\sqrt{\delta}\zeta))a\iota_1^2(\gamma + \kappa) - \alpha c^2\delta\epsilon_1^2)\sqrt{a\alpha(\gamma + \kappa)} c\delta e^{i\Theta}}{(\gamma + \kappa)(\mp c\delta\iota_1\epsilon_1(\cot^2(\sqrt{\delta}\zeta) + 1)\sqrt{a\alpha(\gamma + \kappa)} + \cot(\sqrt{\delta}\zeta)(\delta^{\frac{3}{2}}\alpha c^2\epsilon_1^2 + a\sqrt{\delta}\iota_1^2(\gamma + \kappa)))a}, \delta > 0 \quad (3.36)$$

where,  $\Upsilon = \tanh(\sqrt{-\delta}\zeta)$ ,  $\Pi = \coth(\sqrt{-\delta}\zeta)$ ,  $\Theta = a\frac{x^\sigma}{\sigma} + (2\alpha c^2\delta - \alpha a^2 + \eta a)\frac{t^\sigma}{\sigma}$  and  $\zeta = c\frac{x^\sigma}{\sigma} + (-2\alpha ac + \eta c)\frac{t^\sigma}{\sigma}$ .

Set 7:

$$b = -4\alpha c^2\delta - \alpha a^2 + \eta a, \iota_0 = 0, \epsilon_0 = \pm \frac{\sqrt{\alpha(-4\alpha c^2\delta\epsilon_1^2 + a\gamma\iota_1^2 + a\kappa\iota_1^2)}}{\alpha c}, \tau_1 = \delta\iota_1, \varepsilon_1 = -\delta\epsilon_1$$

Therefore, we get the subsequent analytical solutions:

$$q_7^1 = \pm \frac{\iota_1\delta(\tanh^2(\sqrt{-\delta}\zeta) - 1)\alpha c}{\sqrt{\alpha(a(\gamma + \kappa)\iota_1^2 - 4\alpha c^2\delta\epsilon_1^2)} \sqrt{-\delta} \tanh(\sqrt{-\delta}\zeta) \pm \delta\epsilon_1\alpha c(\tanh^2(\sqrt{-\delta}\zeta) + 1)} e^{i\Theta}, \delta < 0 \quad (3.37)$$

$$q_7^2 = \pm \frac{\iota_1\delta(\coth^2(\sqrt{-\delta}\zeta) - 1)\alpha c}{\sqrt{\alpha(a(\gamma + \kappa)\iota_1^2 - 4\alpha c^2\delta\epsilon_1^2)} \sqrt{-\delta} \coth(\sqrt{-\delta}\zeta) \pm \delta\epsilon_1\alpha c(\coth^2(\sqrt{-\delta}\zeta) + 1)} e^{i\Theta}, \delta < 0 \quad (3.38)$$

$$q_7^3 = \mp \frac{\iota_1(\delta\zeta^2 + 1)\alpha c e^{i\Theta}}{\sqrt{(a(\gamma + \kappa)\iota_1^2 - 4\alpha c^2\delta\epsilon_1^2)\alpha} \zeta \pm \alpha\epsilon_1(\delta\zeta^2 - 1)}, \delta = 0 \quad (3.39)$$

$$q_7^4 = \pm \frac{\iota_1\delta(\tan^2(\sqrt{\delta}\zeta) + 1)\alpha c e^{i\Theta}}{\sqrt{\alpha(a(\gamma + \kappa)\iota_1^2 - 4\alpha c^2\delta\epsilon_1^2)} \sqrt{\delta} \tan(\sqrt{\delta}\zeta) \pm \delta\epsilon_1\alpha c(\tan(\sqrt{\delta}\zeta) - 1)(\tan(\sqrt{\delta}\zeta) + 1)}, \delta > 0 \quad (3.40)$$

$$q_7^5 = \mp \frac{\iota_1\delta(\cot^2(\sqrt{\delta}\zeta) + 1)\alpha c e^{i\Theta}}{\sqrt{\alpha(a(\gamma + \kappa)\iota_1^2 - 4\alpha c^2\delta\epsilon_1^2)} \sqrt{\delta} \cot(\sqrt{\delta}\zeta) \mp \delta\epsilon_1\alpha c(\cot(\sqrt{\delta}\zeta) - 1)(\cot(\sqrt{\delta}\zeta) + 1)}, \delta > 0 \quad (3.41)$$

where  $\Theta = a\frac{x^\sigma}{\sigma} + (-4\alpha c^2\delta - a^2\alpha + a\eta)\frac{t^\sigma}{\sigma}$  and  $\zeta = c\frac{x^\sigma}{\sigma} + (-2\alpha ac + \eta c)\frac{t^\sigma}{\sigma}$ .

#### 4. Results and discussion with graphical representations

The improved tanh method has been effectively employed to attain optical soliton solutions for the perturbed CLL equation. The graphical depictions of wave solutions play a crucial role in elucidating the internal dynamics of complex nonlinear phenomena. In this section, we will explore the characteristics of the traveling wave solutions derived from the CLL equation. We will also examine various types of solitons and their corresponding physical behaviors. Additionally, we have generated 3D, 2D and density plots using MATLAB to visually represent these concepts.

The imaginary part of the solution (3.9) represents a periodic soliton, as shown in figure 1, for  $\sigma = 0.9$ ,  $a = 0.5$ ,  $c = 4$ ,  $\delta = -0.5$ ,  $\alpha = -0.04$ ,  $\gamma = 1$ ,  $\eta = 2$  and  $\kappa = -2$ . The corresponding density plot of the soliton is depicted in figure 1(b). From figure 1(c), it can be observed that the soliton maintains its shape while changing its position with increasing values of the temporal variable.

Figure 2 depicts the configuration of the real slice of the solution (3.10) for specific parameters:  $\sigma = 0.99$ ,  $a = -0.324$ ,  $c = 2$ ,  $\delta = -1$ ,  $\alpha = -0.05$ ,  $\gamma = -2$ ,  $\eta = 2.93$  and  $\kappa = -3$ . It is observed from the figure that the solution describes a compacton. However, as the value of  $\sigma$  decreases, the solution transforms into another soliton (see figure 2(c)).

The behavior of the modulus of the solution (3.13) characterizes a bell-shaped soliton under specific conditions where  $\sigma = 0.999$ ,  $a = 0.51$ ,  $c = 1.12$ ,  $\delta = -0.5$ ,  $\alpha = 0.5$ ,  $\gamma = -0.2$ ,  $\eta = 0.3$  and  $\kappa = -0.3$ . The corresponding density plot of the soliton is illustrated in figure 3(b). Figure 3(c) reveals that the soliton preserves its shape while shifting its position to the right as time increases.

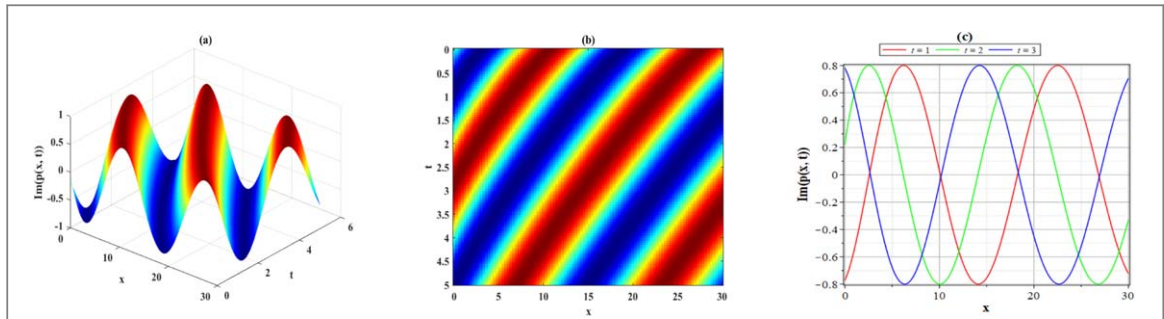


Figure 1. (a) 3D surface plot, (b) density plot and (c) 2D combined plots of imaginary portion of (3.9).

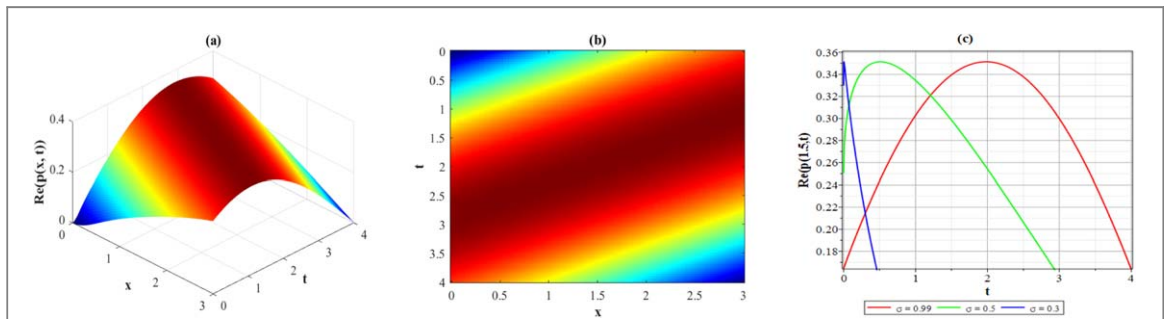


Figure 2. (a) 3D surface plot, (b) density plot and (c) 2D combined plots of real slice of (3.10).

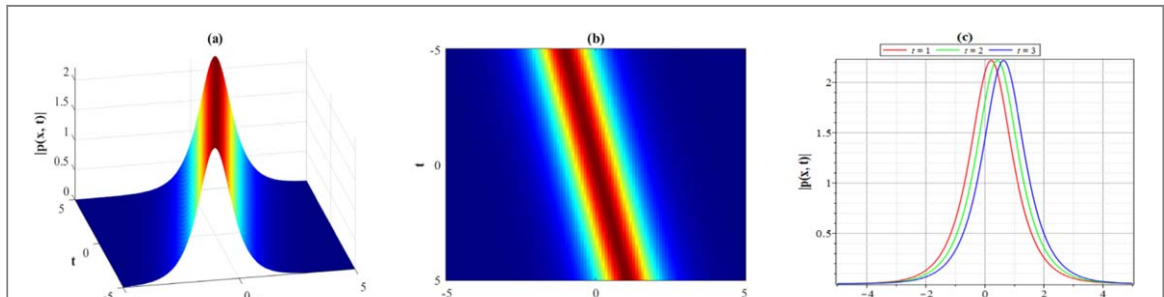


Figure 3. (a) 3D surface plot, (b) density plot and (c) 2D combined plots of the modulus of (3.13).

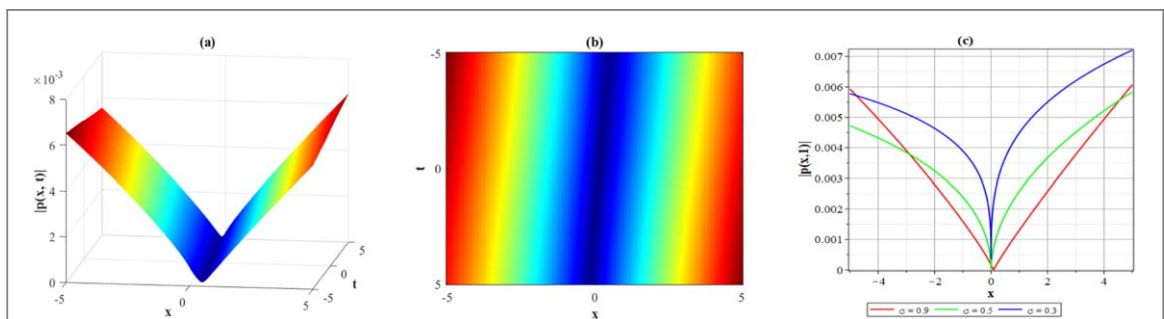


Figure 4. (a) 3D surface plot, (b) density plot and (c) 2D combined plots of the modulus of (3.32).

The absolute value of the solution (3.32) is depicted for specific values:  $\sigma = 0.9$ ,  $a = 0.05$ ,  $c = -0.02$ ,  $\delta = -0.5$ ,  $\alpha = -0.05$ ,  $\gamma = -0.02$ ,  $\eta = 0.083$ ,  $\kappa = -0.003$ ,  $\iota_1 = 0.03$  and  $\epsilon_1 = -0.001$ , as illustrated in figure 4. This solution exhibits a bell-shaped soliton characteristic for the given parameter values. Additionally, it can be noticed from figure 4(c) that lessening the value of  $\sigma$  leads to a spike at the bottom end of the soliton.

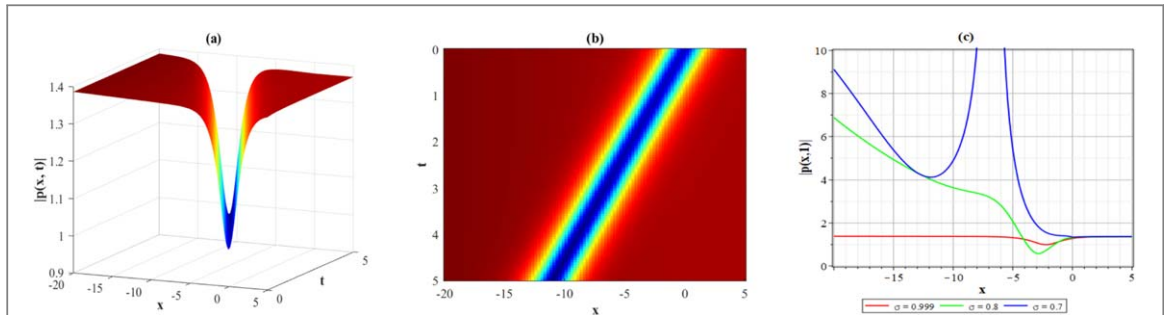


Figure 5. (a) 3D surface plot, (b) density plot and (c) 2D combined plots of the absolute value of (3.33).

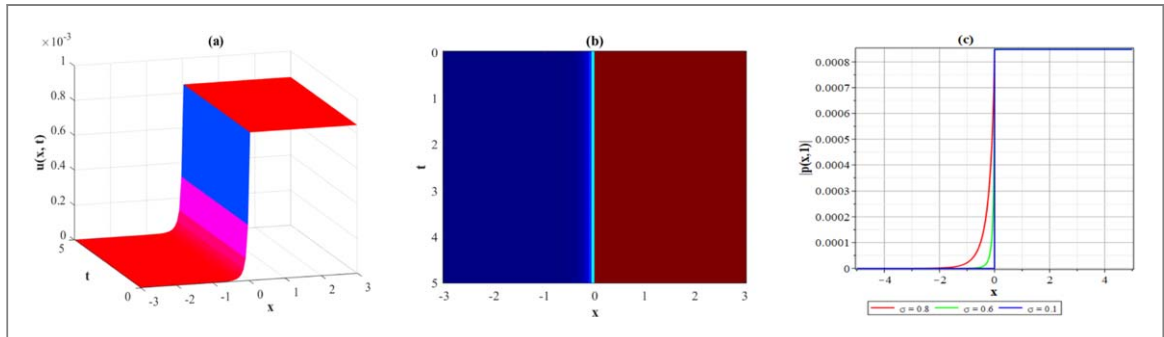


Figure 6. (a) 3D surface plot, (b) density plot and (c) 2D combined plots of the modulus of (3.37).

The absolute value of the solution (3.33) is portrayed in figure 5, which has been generated using appropriate parameters:  $\sigma = 0.999$ ,  $a = -0.2$ ,  $c = 0.5$ ,  $\delta = -1$ ,  $\alpha = 3$ ,  $\gamma = 1$ ,  $\eta = 1$ ,  $\kappa = 1$ ,  $\iota_1 = 1$  and  $\epsilon_1 = 1$ . Furthermore, from the combined 2D plots in figure 5(c), we observe that a slight variation in  $\sigma$  leads to a significant alteration in the wave profile, resulting in structural breakage and the presence of singularities.

Figure 6 displays the configuration of the modulus of solution (3.37), with appropriate parameter values:  $\sigma = 0.6$ ,  $a = 5$ ,  $c = 0.001$ ,  $\delta = -0.0004$ ,  $\alpha = 0.75$ ,  $\gamma = -0.1$ ,  $\eta = -1$ ,  $\kappa = -0.03$ ,  $\iota_1 = 0.0085$  and  $\epsilon_1 = -10$ . The figure portrays a kink soliton having non-smoothness at upper part. It is noteworthy from figure 6(c) that the solution (3.37) tends to lose its smoothness in the lower part as the value of  $\sigma$  decreases.

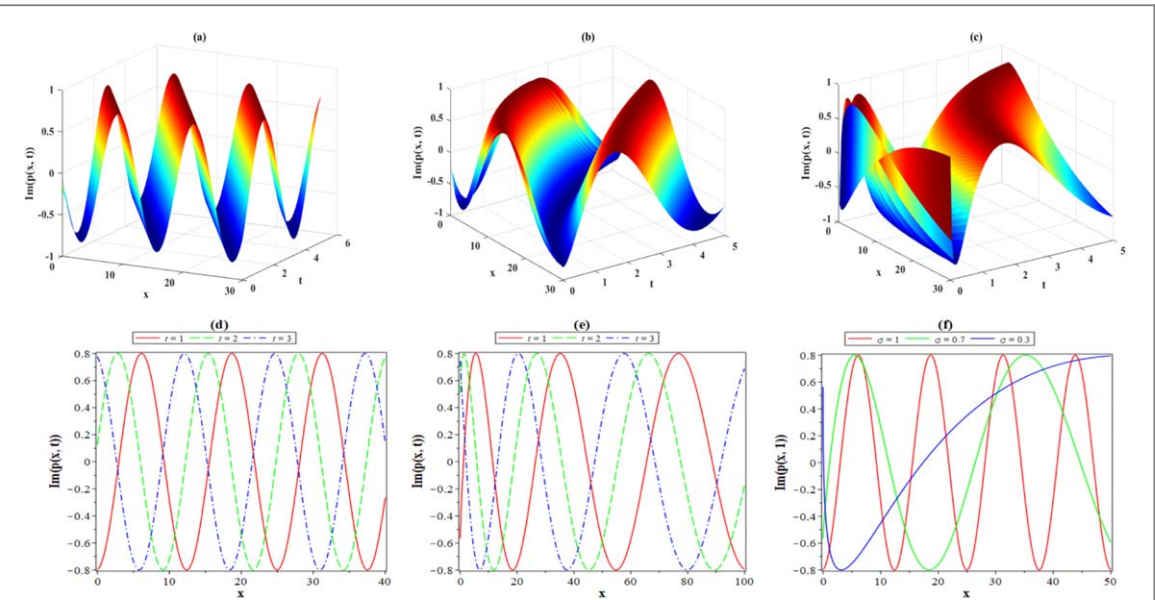
#### 4.1. Effects of fractional derivative order

In this subsection, we have visualized how the fractional derivative order affects the solutions by plotting 3D and 2D graphs of the obtained solutions for various values of  $\sigma$ . By delving into the examination of the influence of  $\sigma$ , we aim to offer valuable insights into the dynamics of waves.

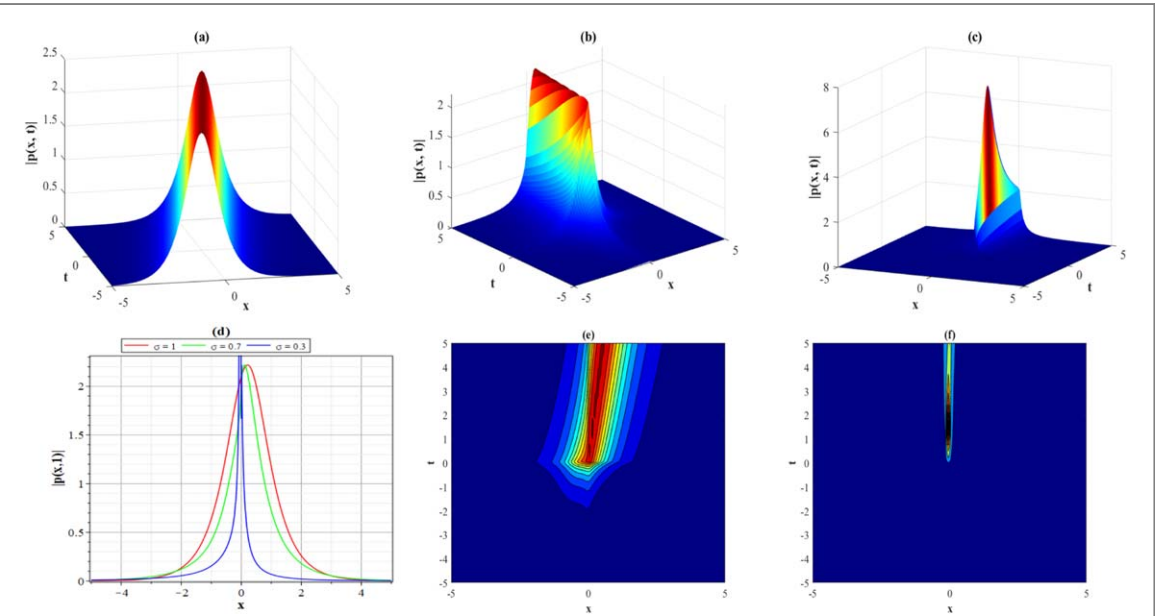
Figure 7 is portrayed for appropriate values of  $a=0.5$ ,  $c=4$ ,  $\delta=-0.5$ ,  $\alpha=-0.04$ ,  $\gamma=1$ ,  $\eta=2$ ,  $\kappa=-2$ , which displays the physical characteristics of imaginary slice of the solution (3.9). When  $\sigma=1$ , solution (3.9) exhibits a periodic soliton. However, decreasing the value of  $\sigma$  will cause the wavelength to broaden, and at  $\sigma=0.3$ , it will no longer qualify as a periodic soliton. Again, from figures 7(d) and (e), it can be observed that the wave exhibits non-regular oscillatory behavior for  $\sigma=0.7$ , whereas this behavior does not occur for the integer case, i.e., when  $\sigma=1$ .

Figure 8 depicts the physical feature of the modulus of solution (3.13) for appropriate parameter values:  $a=0.51$ ,  $c=1.12$ ,  $\delta=-0.5$ ,  $\alpha=0.5$ ,  $\gamma=-0.2$ ,  $\eta=0.3$  and  $\kappa=-0.3$ . For  $\sigma=1$ , the solution (3.13) represents a bell-shaped (bright) soliton. However, as the value of  $\sigma$  decreases, the soliton tends to lose its smoothness, and at  $\sigma=0.3$ , the solution becomes a singular bell soliton. Figures 8(e) and (f) are the corresponding contour plots of 8(b) and (c), respectively. Contour plots provide a visual representation of complex wave data, allowing us to quickly grasp the spatial distribution and variation of wave parameters such as amplitude, frequency, and phase.

Analogously, the influence of fractional derivative order on alternative solutions can be demonstrated in a similar manner. It can be observed that the effect on the propagating waves increases with the decreasing order of the fractional derivative. This characterization provides comprehensive information about these propagating waves, resulting in a significant enhancement in various related applications.



**Figure 7.** (a) 3D surface plot for  $\sigma = 1$ , (b) 3D surface plot for  $\sigma = 0.7$ , (c) 3D surface plot for  $\sigma = 0.3$ , (d) 2D plots for  $\sigma = 1$ , (e) 2D plots for  $\sigma = 0.7$  and (d) 2D combined plots of the imaginary portion of solution (3.9).



**Figure 8.** (a) 3D surface plot for  $\sigma = 1$ , (b) 3D surface plot for  $\sigma = 0.7$ , (c) 3D surface plot for  $\sigma = 0.3$ , (d) 2D combined plots, (e) contour for  $\sigma = 0.7$  and (f) contour for  $\sigma = 0.3$  of the absolute value of solution (3.13).

## 5. Results' comparison

Various researchers have explored the Chen-Lee-Liu model using different methods, as discussed earlier in the introduction section. In this section, we will compare the solutions obtained for the CLL equation with those presented by Martínez *et al* [25]. Martínez *et al*. applied the modified exp  $(-\phi(\xi))$ -expansion function method (MEFM) to the fractional perturbed Chen-Lee-Liu nonlinear equation and obtained trigonometric and hyperbolic solutions similar to those obtained by our proposed technique. Again, we obtained seven sets of solutions, whereas Martínez *et al* obtained only three sets by considering different cases. Furthermore, based on our obtained analytical solutions and those given by Martínez *et al* [25], we make a comparison which is demonstrated in table 1. Hence, it becomes evident that some of the acquired solutions align with those from previous studies under suitable configurations of arbitrary parameters, while others are novel and standard. Moreover, the fundamental structures of the resulting solutions, delineated through this method, are comprehensive.

**Table 1.** Comparison between Martínez *et al* [25] solutions and our solutions.

| Results of Martínez <i>et al</i> [25]   | Results obtained in this article   |
|---|--|
| If we put $\theta = \gamma, K = -1$ and $\sigma = \kappa$ in solution $q_3(z, t)$ and $q_{13}(z, t)$ , we can write them in a simplified form as:<br>$q_3(z, t) = \pm C_1 \frac{\text{Acoth}(\Lambda \zeta)}{\sqrt{\gamma + \kappa}} e^{i\Psi}$ and $q_{13}(z, t) = \pm C_2 \frac{\text{Acoth}(\Lambda \zeta)}{\sqrt{\gamma + \kappa}} e^{i\Psi}$ , where $C_1$ and $C_2$ are arbitrary constant. | If we put $c = a = 1$ , the solution (3.18) can be written as:<br>$q_3^2(x, t) = M_1 \frac{\sqrt{-\delta} \coth(\sqrt{-\delta} \zeta)}{\sqrt{\gamma + \kappa}} e^{i\Theta}$ , where $M_1$ is arbitrary constant. |
| If we put $\theta = \gamma, K = -1$ and $\sigma = \kappa$ in solution $q_5(z, t)$ and $q_{15}(z, t)$ , we can write in a simplified form as:<br>$q_5(z, t) = \pm \frac{C_3}{\xi \sqrt{\gamma + \kappa}} e^{i\Psi}$ and<br>$q_{15}(z, t) = \pm \frac{C_4}{\xi \sqrt{\gamma + \kappa}} e^{i\Psi}$ , where $C_3$ and $C_4$ areis arbitrary constant.   | If we put $c = a = 1$ , the solution (3.18) can be written as:<br>$q_3^3(x, t) = \frac{M_2}{\zeta \sqrt{\gamma + \kappa}} e^{i\Theta}$ , where $M_2$ is arbitrary constant.                                      |

## 6. Conclusion

In this investigation, utilizing the suggested improved tanh method and the definition of conformable derivative, we have successfully achieved and symbolically derived numerous new exact traveling wave solutions to the space-time fractional nonlinear perturbed Chen-Lee-Liu equation. The suggested approach is highly efficient, reliable, and potent. It eliminates the need for linearization, perturbation, initial conditions, and boundary conditions, thereby underscoring one of its key advantages. We have uncovered closed-form solutions for the mentioned equation, along with configurations such as periodic, bell-shaped, anti-bell-shaped, V-shaped, kink, and compacton, employing diverse sets of free parameters. These findings are illustrated through 3-D, density, and 2-D plots. It is noteworthy that the accuracy of all derived solutions is verified by directly substituting them back into the original equations. The referenced CLL equation holds importance in both communication through optical fibers and the study of plasma physics. The obtained solutions could offer significant assistance, and the approach considered here may be utilized in future research to identify solitary wave solutions for nonlinear problems that arise in theoretical physics, applied mathematics, and other areas of non-linear sciences.

## Acknowledgments

The authors wish to extend their gratitude to the anonymous referees for their valuable feedback and suggestions that have contributed to the enhancement of this article.

## Data availability statement

No new data were created or analysed in this study.

## Funding statement

No funding was used in this study.

## ORCID iDs

Aminul Islam  <https://orcid.org/0009-0005-2877-7975>  
Md. Sagib  <https://orcid.org/0009-0002-9945-3458>

## References

- [1] Ali K K, Yusuf A and Ma W X 2023 Dynamical rational solutions and their interaction phenomena for an extended nonlinear equation *Commun. Theor. Phys.* **75** 035001
- [2] Ali K K, Osman M S and Abdel-Aty M 2020 New optical solitary wave solutions of Fokas-Lenells equation in optical fiber via Sine-Gordon expansion method *Alexandria Engineering Journal* **1** 1191–6
- [3] Kundu P R, Fahim M R A, Islam M E and Akbar M A 2021 The sine-Gordon expansion method for higher-dimensional NLEEs and parametric analysis *Helijon* **7** e06459
- [4] Lu B 2012 The first integral method for some time fractional differential equations *J. Math. Anal. Appl.* **15** 684–93

[5] Eslami M and Rezazadeh H 2016 The first integral method for Wu-Zhang system with conformable time-fractional derivative *Calcolo* **53** 475–85

[6] Akbulut A and Kaplan M 2018 Auxiliary equation method for time-fractional differential equations with conformable derivative *Comput. Math. Appl.* **1** 876–82

[7] Dimitrova Z I and Vitanov K N 2021 Homogeneous balance method and auxiliary equation method as particular cases of simple equations method (SEsM) *In AIP Conference Proceedings* (Constantin and Helena, Bulgaria: AIP Publishing LLC) 2321 030004 (<https://doi.org/10.1063/5.0043070>)

[8] Bekir A 2008 New solitons and periodic wave solutions for some nonlinear physical models by using the sine-cosine method *Physica Scripta* **3** 045008

[9] Yao S W, Behera S, Inc M, Rezazadeh H, Virdi J P, Mahmoud W, Arqub O A and Osman M S 2022 Analytical solutions of conformable Drinfel'd-Sokolov-Wilson and Boiti Leon Pempinelli equations via sine-cosine method *Results in Physics* **42** 105990

[10] Barman H K, Roy R, Mahmud F, Akbar M A and Osman M S 2021 Harmonizing wave solutions to the Fokas-Lenells model through the generalized Kudryashov method *Optik* **229** 166294

[11] Gaber A A, Aljohani A F, Ebaid A and Machado J T 2019 The generalized Kudryashov method for nonlinear space-time fractional partial differential equations of burgers type *Nonlinear Dyn.* **95** 361–8

[12] Bian C, Pang J, Jin L and Ying X 2010 Solving two fifth order strong nonlinear evolution equations by using the GG'-expansion method *Commun. Nonlinear Sci. Numer. Simul.* **15** 2337–43

[13] Akçağlı Ş and Aydemir T 2016 Comparison between the  $(G'/G)$ -expansion method and the modified extended tanh method *Open Physics* **14** 88–94

[14] Fan E 2000 Extended tanh-function method and its applications to nonlinear equations *Physics Letters A* **277** 212–8

[15] Abazari R 2014 Application of extended tanh function method on KdV-Burgers equation with forcing term *Rom. J. Phys.* **59** 3–11

[16] Ali K K, Tarla S, Yusuf A and Yilmazer R 2023 Closed form wave profiles of the coupled-Higgs equation via the  $\Phi^6$ -model expansion method *Int. J. Mod. Phys. B* **37** 2350070

[17] Tarla S, Ali K K, Yilmazer R and Yusuf A 2022 Investigation of the dynamical behavior of the Hirota-Maccari system in single-mode fibers *Opt. Quantum Electron.* **54** 613

[18] Tarla S, Ali K K, Yilmazer R and Yusuf A 2022 New behavior of tsunami and tidal oscillations for Long-and short-wave interaction systems *Modern Physics Letters B* **36** 2250116

[19] He J H and Wu X H 2006 Exp-function method for nonlinear wave equations *Chaos, Solitons Fractals* **30** 700–8

[20] Yokus A, Durur H, Ahmad H, Thounthong P and Zhang Y F 2020 Construction of exact traveling wave solutions of the bogoyavlenskii equation by  $(G'/G)$ ,  $1/G$ -expansion and  $(1/G')$ -expansion techniques *Results in Physics* **19** 103409

[21] Akbulut A, Kaplan M and Tascan F 2016 Conservation laws and exact solutions of Phi-four (Phi-4) equation via the  $(G'/G)$ ,  $1/G$ -expansion method *Zeitschrift für Naturforschung A* **71** 439–46

[22] Shallal M A, Ali K K, Raslan K R, Rezazadeh H and Bekir A 2020 Exact solutions of the conformable fractional EW and MEW equations by a new generalized expansion method *Journal of Ocean Engineering and Science* **5** 223–9

[23] Akbulut A and Taşcan F 2017 Application of conservation theorem and modified extended tanh-function method to (1,1)-dimensional nonlinear coupled Klein-Gordon-Zakharov equation *Chaos, Solitons Fractals* **104** 33–40

[24] Alam L M and Jiang X 2021 Exact and explicit traveling wave solution to the time-fractional phi-four and (2,1) dimensional CBS equations using the modified extended tanh-function method in mathematical physics *Partial Differential Equations in Applied Mathematics* **4** 100039

[25] Yépez-Martínez H, Rezazadeh H, Inc M and Ali Akinlar M 2021 New solutions to the fractional perturbed Chen-Lee-Liu equation with a new local fractional derivative *Waves Random Complex Medium* **20** 1–36

[26] Wang X B and Han B 2021 Pure soliton solutions of the nonlocal Kundu-nonlinear Schrödinger equation *Theor. Math. Phys.* **206** 40–67

[27] Li Y, Hu B, Zhang L and Li J 2024 The exact solutions for the nonlocal Kundu-NLS equation by the inverse scattering transform *Chaos, Solitons Fractals* **180** 114603

[28] Hu B, Zhang L and Zhang N 2021 On the Riemann-Hilbert problem for the mixed Chen-Lee-Liu derivative nonlinear Schrödinger equation *J. Comput. Appl. Math.* **390** 113393

[29] Ozisik M, Bayram M, Sefer A and Cinar M 2022 Optical soliton solutions of the Chen-Lee-Liu equation in the presence of perturbation and the effect of the inter-modal dispersion, self-steepening and nonlinear dispersion *Opt. Quantum Electron.* **54** 792

[30] Khatun M M and Akbar M A 2023 New optical soliton solutions to the space-time fractional perturbed Chen-Lee-Liu equation *Results in Physics* **46** 106306

[31] Mohamed M S, Akinyemi L, Najati S A and Elagan S K 2022 Abundant solitary wave solutions of the Chen-Lee-Liu equation via a novel analytical technique *Opt. Quantum Electron.* **54** 141

[32] Arnows A H, Mirzazadeh M, Akbulut A and Akinyemi L 2022 Optical solutions and conservation laws of the chen-lee-liu equation with kudryashov's refractive index via two integrable techniques *Waves Random Complex Medium* **10** 1–7

[33] Islam S R, Khan K and Akbar M A 2023 Optical soliton solutions, bifurcation, and stability analysis of the Chen-Lee-Liu model *Results in Physics* **51** 106620

[34] Murad M A, Hamasalh F K and Ismael H F 2023 Time-fractional chen-lee-liu equation: various optical solutions arising in optical fiber *Journal of Nonlinear Optical Physics & Materials* **13** 2350061

[35] El-Shiekh R M and Gaballah M 2024 Novel optical waves for the perturbed nonlinear chen-lee-liu equation with variable coefficients using two different similarity techniques *Alexandria Engineering Journal* **86** 548–55

[36] Zhang Y and Lin B 2024 The riemann-hilbert approach for the chen-lee-liu equation and collisions of multiple solitons *Nonlinear Dyn.* **112** 3737–48

[37] Tripathy A and Sahoo S 2022 New distinct optical dynamics of the beta-fractionally perturbed chen-lee-liu model in fiber optics *Chaos, Solitons Fractals* **163** 112545

[38] Ouahid L, Alanazi M M, Shahrani J S, Abdou M A and Kumar S 2023 New optical soliton solutions and dynamical wave formations for a fractionally perturbed chen-lee-liu (CLL) equation with a novel local fractional (NLF) derivative *Mod. Phys. Lett. B* **37** 2350089

[39] Islam M T, Sarkar T R, Abdulla F A and Gómez-Aguilar J F 2023 Characteristics of dynamic waves in incompressible fluid regarding nonlinear boiti-leon-manna-pempinelli model *Phys. Scr.* **98** 085230

[40] Islam M T, Akter M A, Gomez-Aguilar J F, Akbar M A and Pérez-Careta E 2023 Innovative and diverse soliton solutions of the dual core optical fiber nonlinear models via two competent techniques *Journal of Nonlinear Optical Physics & Materials* **32** 2350037

[41] Khalil R, Al Horani M, Yousef A and Sababheh M 2014 A new definition of fractional derivative *J. Comput. Appl. Math.* **264** 65–70